Mebendazolium mesylate anhydride salt: rational design based on supramolecular assembly, synthesis, and solid-state characterization

Eduardo L. Gutiérrez,*[a] Agustín A. Godoy [b]†, Elena V. Brusau [b], Daniel Vega [c], Griselda E. Narda [b], Sebastián Suárez [d] and Florencia Di Salvo [d]

a. INQUISAL–CONICET, Área de Química Física, Facultad de Química, Bioquímica y Farmacia, Universidad Nacional de San Luis, Chacabuco y Pedernera, CP 5700, San Luis, Argentina.

b. Instituto de Investigaciones en Tecnología Química (INTEQUI), Área de Química General e Inorgánica "Dr. G. F. Puelles", Facultad de Química, Bioquímica y Farmacia, Universidad Nacional de San Luis, Almte. Brown 1500-1402, D5700APA, Chacabuco y Pedernera, CP 5700, San Luis, Argentina.

c. Gerencia de Investigación y Aplicaciones, Centro Atómico Constituyentes, Comisión Nacional de Energía Atómica, Av. Gral. Paz 1499, 1650 San Martín, Buenos Aires, Argentina.

d. INQUIMAE-CONICET y Departamento de Química Inorgánica, Analítica y Química Física, Facultad de Ciencias Exactas y Naturales, Universidad de Buenos Aires, CABA, Argentina.

† Present address: Departamento de Física de la Materia Condensada, Instituto de Nanociencia y Nanotecnología, Centro Atómico Constituyentes, Comisión Nacional de Energía Atómica (CNEA), Avenida General Paz 1499, (1650) San Martín, Buenos Aires, Argentina.

** egutierrez@unsl.edu.ar*

Electronic Supplementary Information (ESI)

Introduction

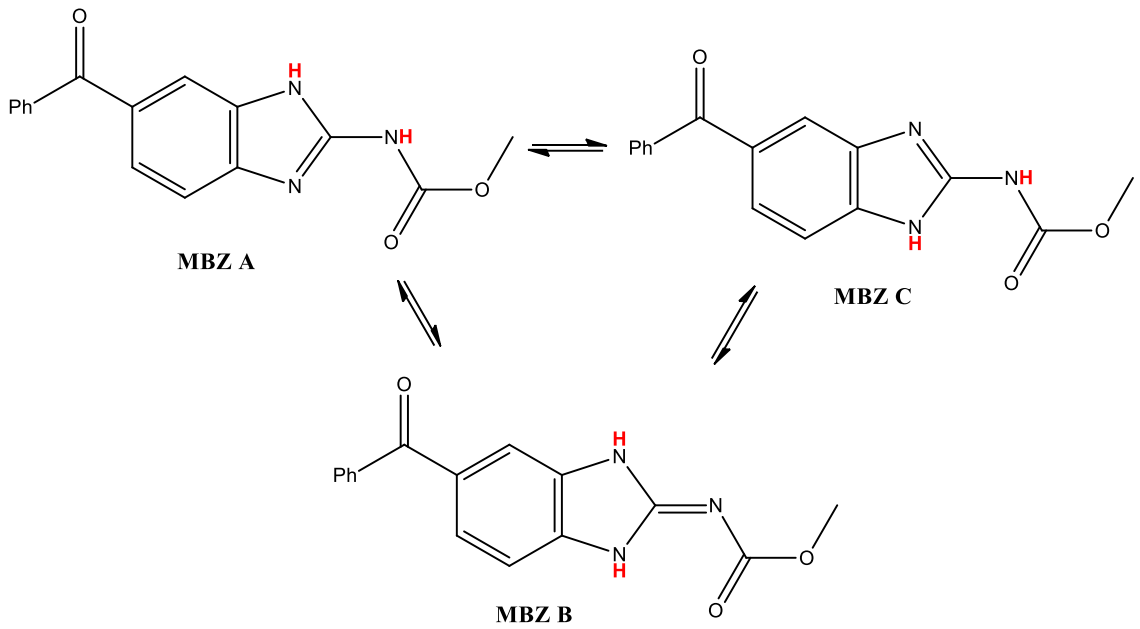

Scheme S1. Tautomeric equilibria between the three tautomers found in MBZ A, MBZ B, and MBZ C desmotropes respectively.

Experimental

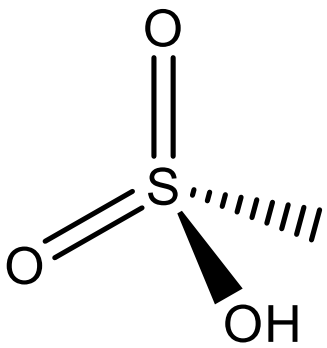

Scheme S2. Methanesulfonic acid molecular structure (MsOH).

Results and discussion

Table S1. MBZ···MBZ $R_2^2(8)$ homosynthon found in MBZ A.

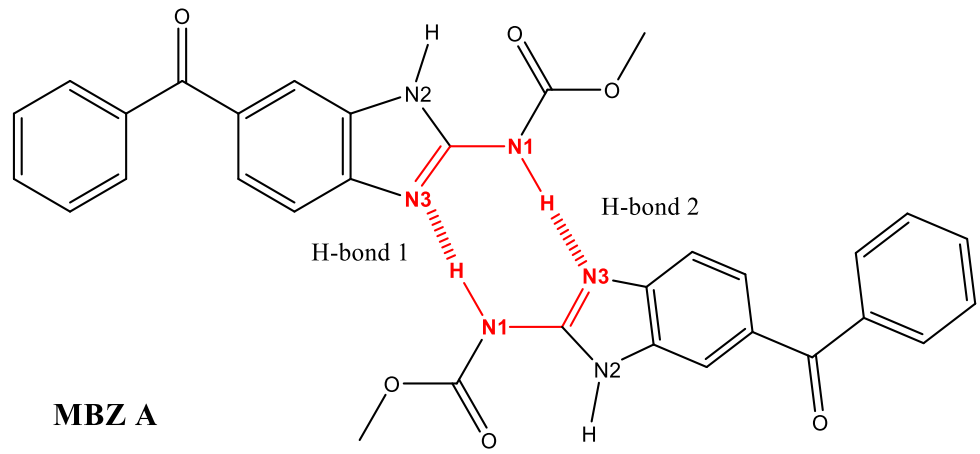

	H-bond 1		H-bond 2	
	A···H / Å	**A···D / Å**	**A···H / Å**	**A···D / Å**
MBZ A [A]	2.1	2.86(3)	2.1	2.86(3)

[A] F. F. Ferreira, S. Antonio Gutierrez, P. C. Pires Rosa and C. de O. Paiva-Santos, *Int. J. Drug Dev. Res.*, 2011, **3**, 26–33. (CCDC deposition number: 736731).

Table S2. MBZ···MBZ $R_2^2(8)$ homosynthon found in MBZ B.

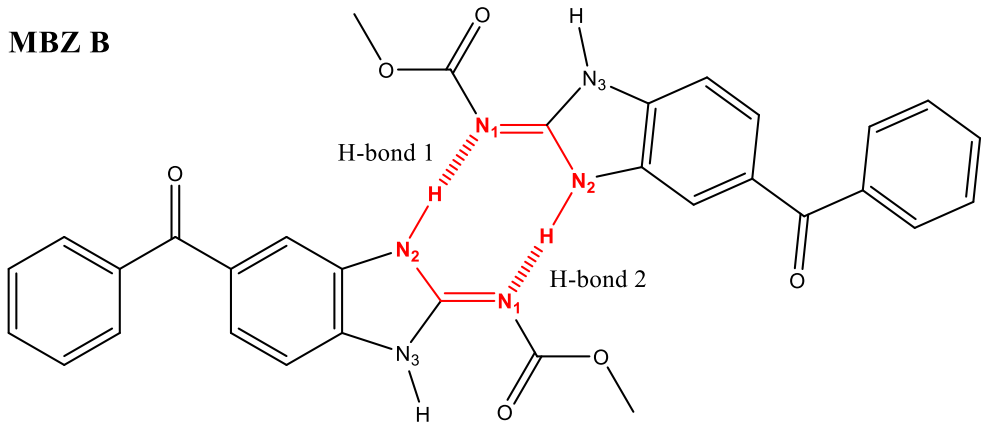

	H-bond 1		H-bond 2	
	A···H / Å	**A···D / Å**	**A···H / Å**	**A···D / Å**
MBZ B [B]	1.92	2.992(9)	1.92	2.992(9)

[B] F. Bravetti, S. Bordignon, E. Alig, D. Eisenbeil, L. Fink, C. Nervi, R. Gobetto, M. U. Schmidt, and M. R. Chierotti, *Chem. Eur. J.*, 2021, **98**, e202103589. (CCDC deposition number: 2095820).

Table S3. MBZ···MBZ $R_2^2(8)$ homosynthon found in MBZ C.

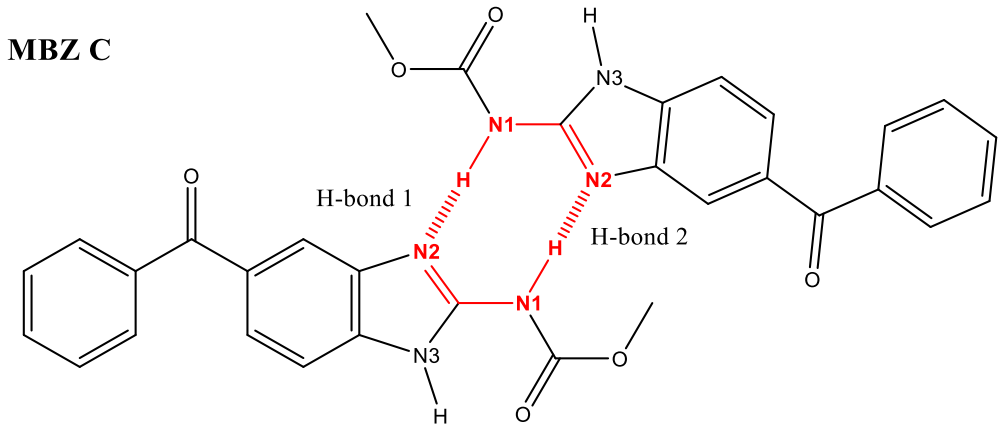

	H-bond 1		H-bond 2	
	A···H / Å	**A···D / Å**	**A···H / Å**	**A···D / Å**
MBZ C [c]	1.99	2.872(8)	1.99	2.872(8)

[c] F. T. Martins, P. P. Neves, J. Ellena, G. E. Camí, E. V. Brusau and G. E. Narda, *J. Pharm. Sci.*, 2009, **98**, 2336–2344. (CCDC deposition number: 690724).

Table S4

Conformational parameters involved in the formation of heterosynthons I and II (CCDC deposition number)

Mebendazolium salts	**C3–N1 / Å**	**α / °**	**β / °**	**γ / °**	**δ / °**	**ε / °**
Reference parameters	**1.37(1)**	**120**	**120**	**120**	**0**	**120** **109.5**
Nitrate[1] (I) (1585622)	1.349(3)	123.3(2)	118	118	–1.4(4)	120.2(3)
Perchlorate[2] (I) (1995782)	1.341(6)	123.5(4)	118	118	2.7(7)	110.0(2)
Methylsulfate[2] (I) (1995783)	1.341(3)	123.0(2)	118	119	0.5(4)	113.6(1)
Mesylate anhydride (I) (this work)	1.348(10)	124.3(7)	118	118	1.5(13)	111.6(3)
Methanoate[3] (I) (929536)	1.356(5)	123.0(4)	118	119	6.2(7)	126.5(5)
	1.333(6)	122.9(4)	119	119	–2.0(7)	125.2(5)
	1.348(6)	123.2(4)	118	118	–0.8(7)	126.3(5)
Methyloxalate (I)[4] (866968)	1.357(4)	123.7(3)	122	114	3.4(5)	127.7(3)
Trifluoroacetate (II)[3] (929535)	1.347(3)	122.5(2)	119	119	–0.3(4)	129.9(2)
Maleate (II)[4] (866969)	1.360(4)	122.7(3)	123.6	113.5	–5.3(6)	123.6(3)
	1.361(4)	120.8(3)	122	117	–4.8(5)	

Table S5
Hydrogen bonds found in mebendazolium salts with non-carboxylic oxyanions (CCDC deposition number)

Mebendazolium salts	N1–**H**···**O5**	N2–**H**···**O4**	Bifurcated *H*-bonds		C6–**H**···**O4** and/or C6–**H**···**O6**
			N3–**H**···**O2**	N3–**H**···**O6**	
Nitrate[1] (1585622)	2.08 Å	1.87 Å	2.24 Å	2.00 Å	– / –
Perchlorate[2] (1995782)	2.04 Å	1.94 Å	2.19 Å	2.14 Å	2.68 Å / –
Methylsulfate[2] (1995783)	1.89 Å	1.90 Å	2.21 Å	2.04 Å	2.62 Å / –
Mesylate monohydrate[5] (934635)	1.75 Å	-	2.12 Å	1.96 Å	– / 2.62 Å
Mesylate anhydride (this work)	1.87 Å	1.96 Å	2.21 Å	2.00 Å	2.66 Å / 2.69 Å

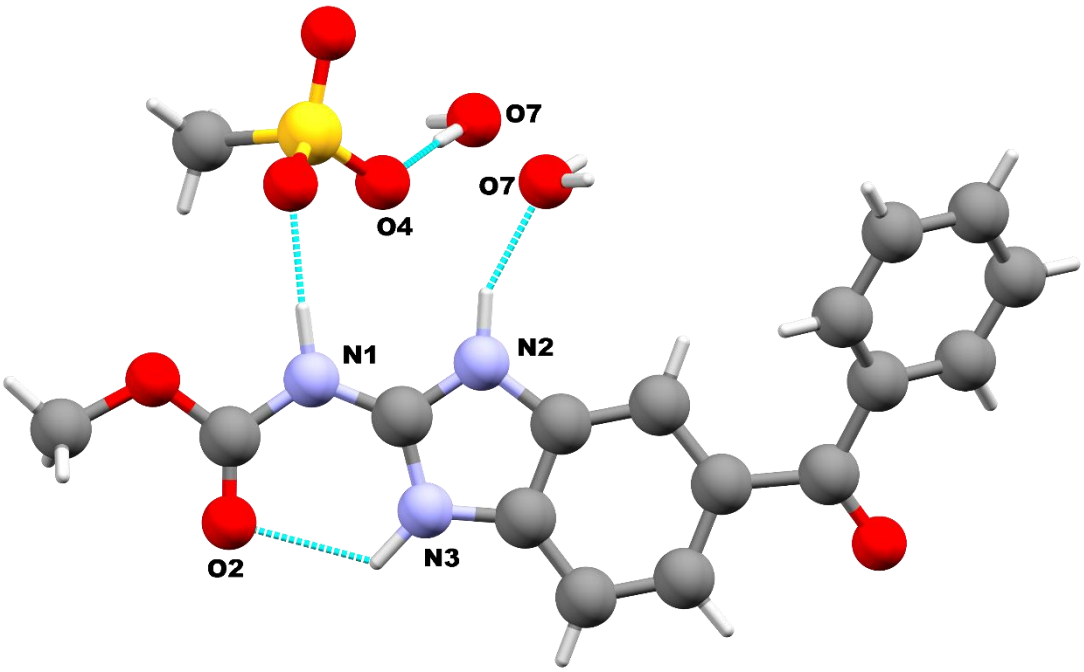

Figure S1. Intermolecular hydrogen bonds found in mebendazolium mesylate monohydrate salt. Color code: carbon (grey), oxygen (red), nitrogen (purple), sulfur (yellow) and hydrogen (white).

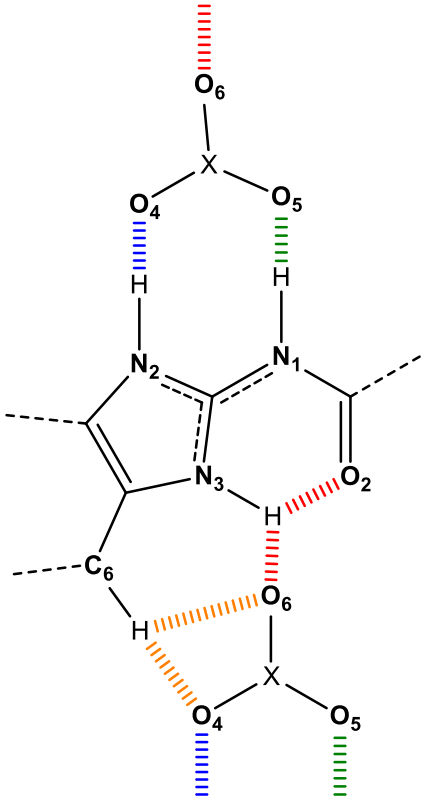

Scheme S3. Extended heterosynthon found in mebendazolium salts with non-carboxylic oxyanions (*i.e.*: nitrate[1] –CCDC 1585622–, perchlorate[2] –CCDC 1995782–, and methylsulfate[2] –1995783–) stabilized by three intermolecular hydrogen bonds.

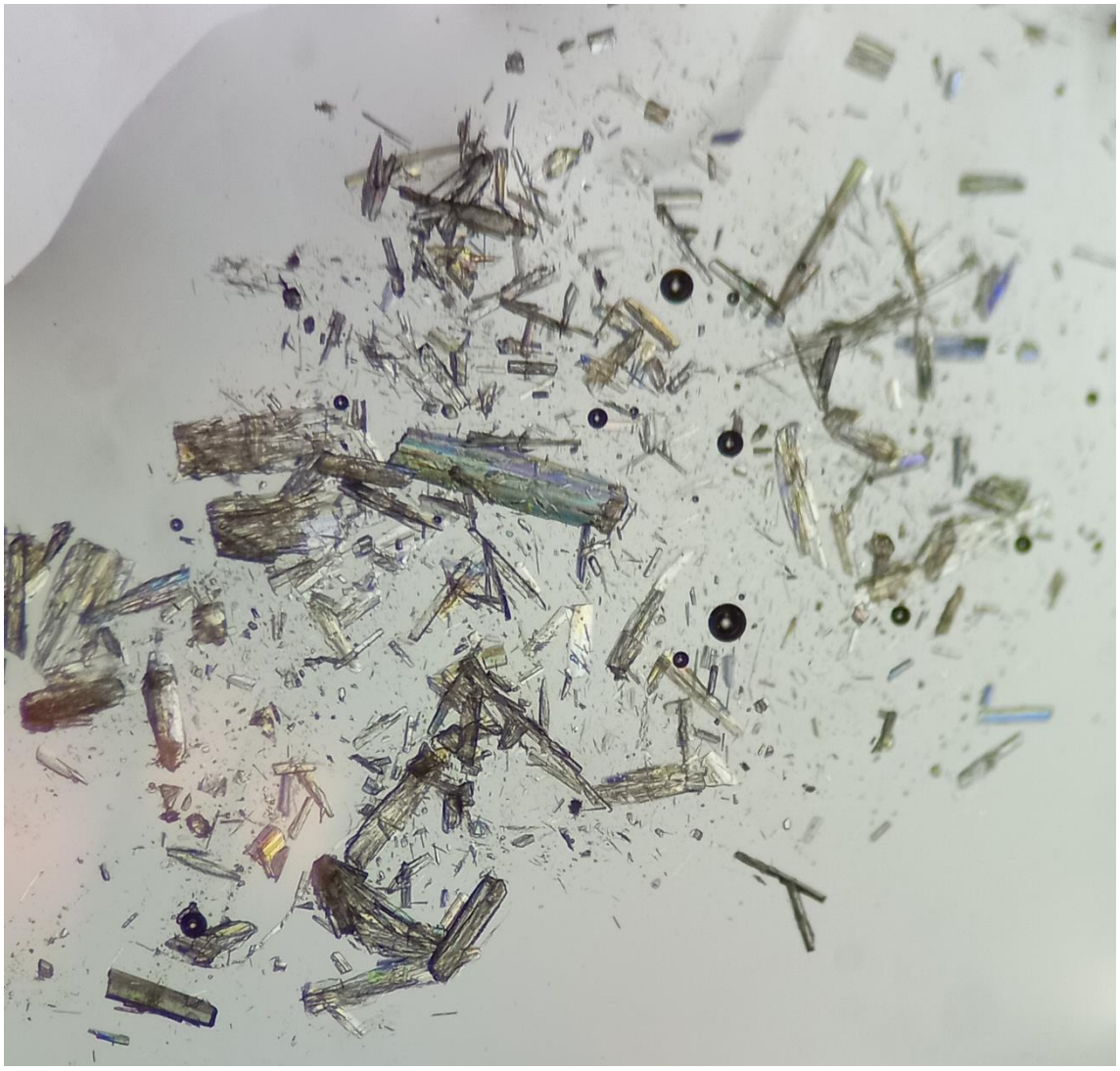

Figure S2. The new solid material as seen under a polarized microscope.

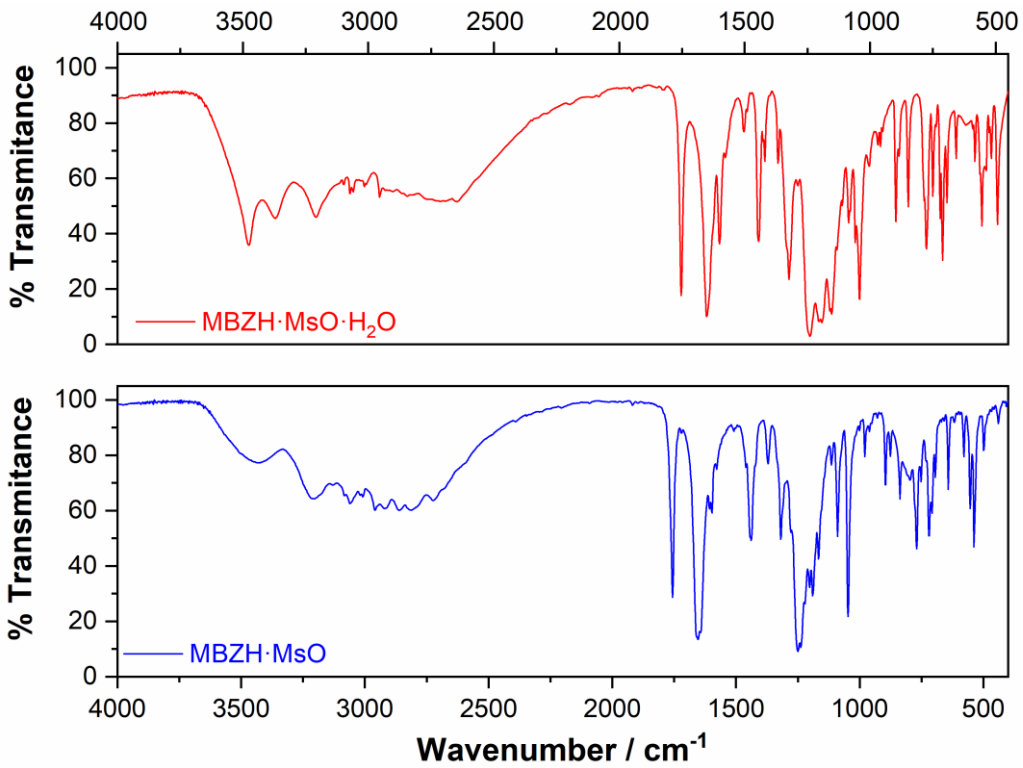

Figure S3. FT-IR spectra of the mebendazolium mesylate monohydrate salt (top) and the mebendazolium mesylate anhydrous salt (bottom).

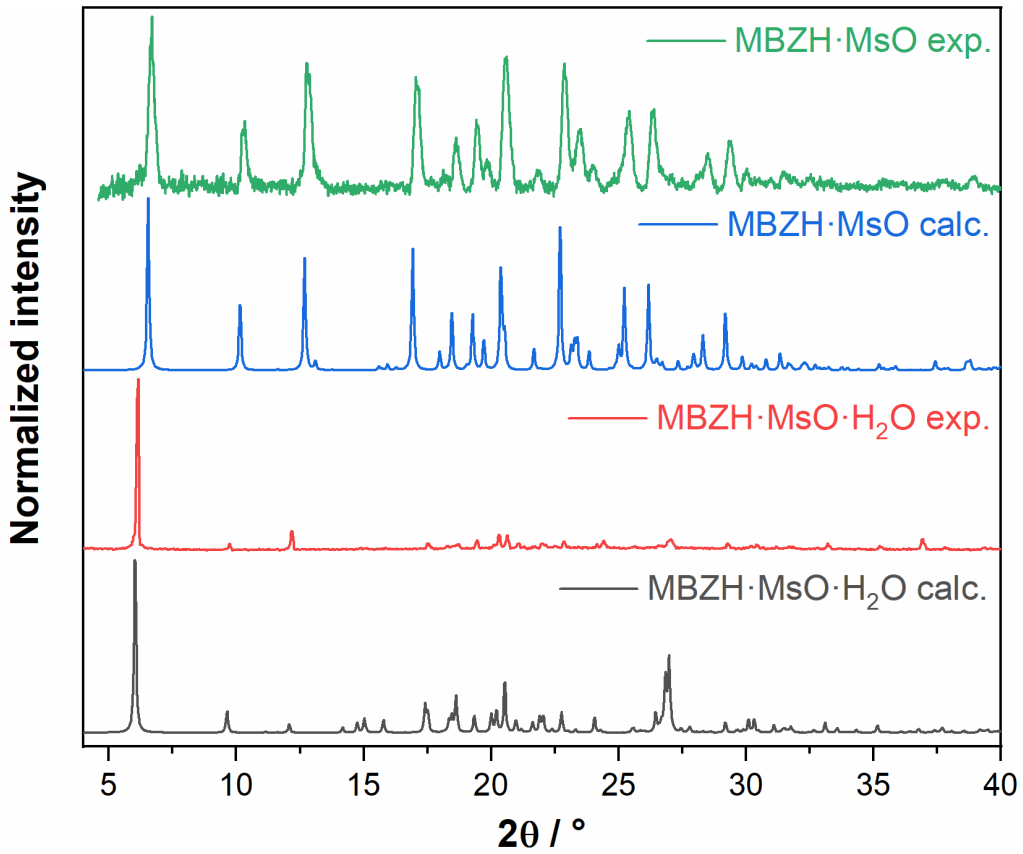

Figure S4. Experimental powder X-ray diffraction patterns of MBZH·MsO and MBZH·MsO·H_2O compared with those calculated from the solved structures.

MBZ (as in polymorph C)

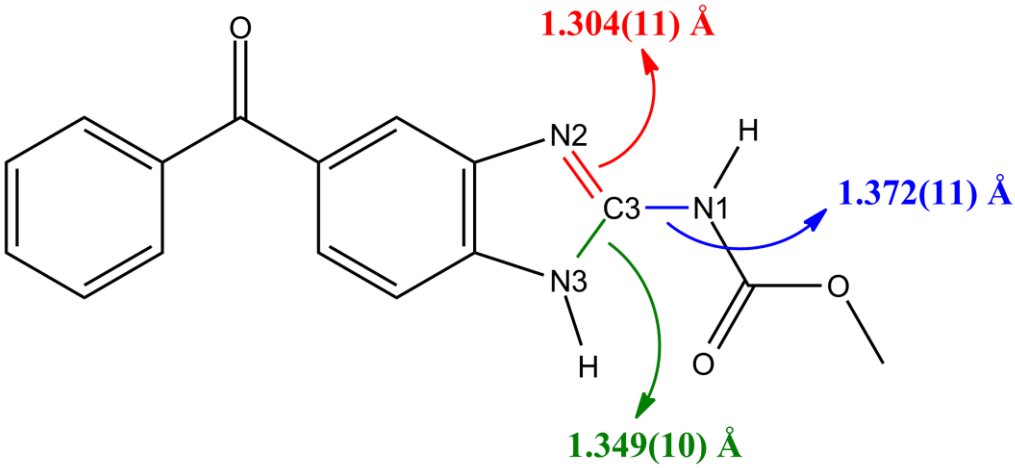

MBZH$^+$ (as in mesylate salt)

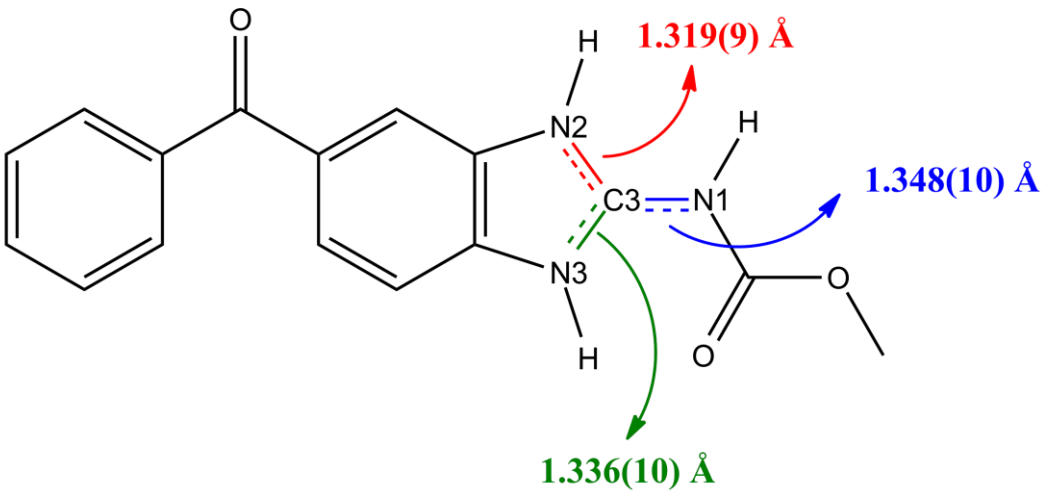

Scheme S4. Effect of protonation on bond lengths of MBZ molecule/ion.

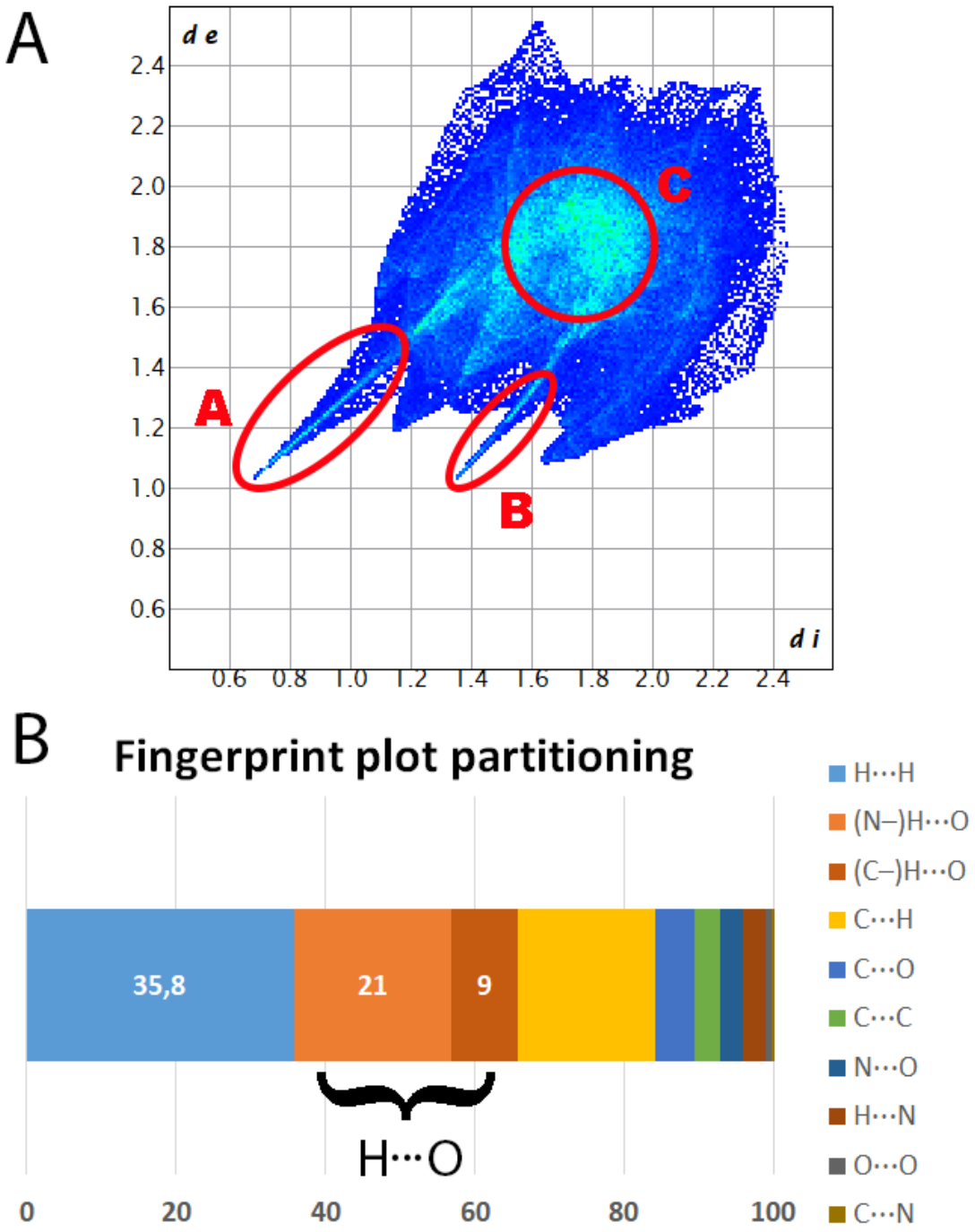

Figure S5. A. 2D-fingerprint plot of MBZH·MsO. **B.** Histogram representing the relative areas of the d_{norm} surface partitioned between the different types of close contact interactions.

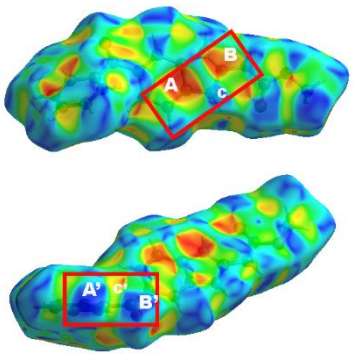

Figure S6. Hirshfeld surface of MBZH⁺ cation mapped with the shape index function.

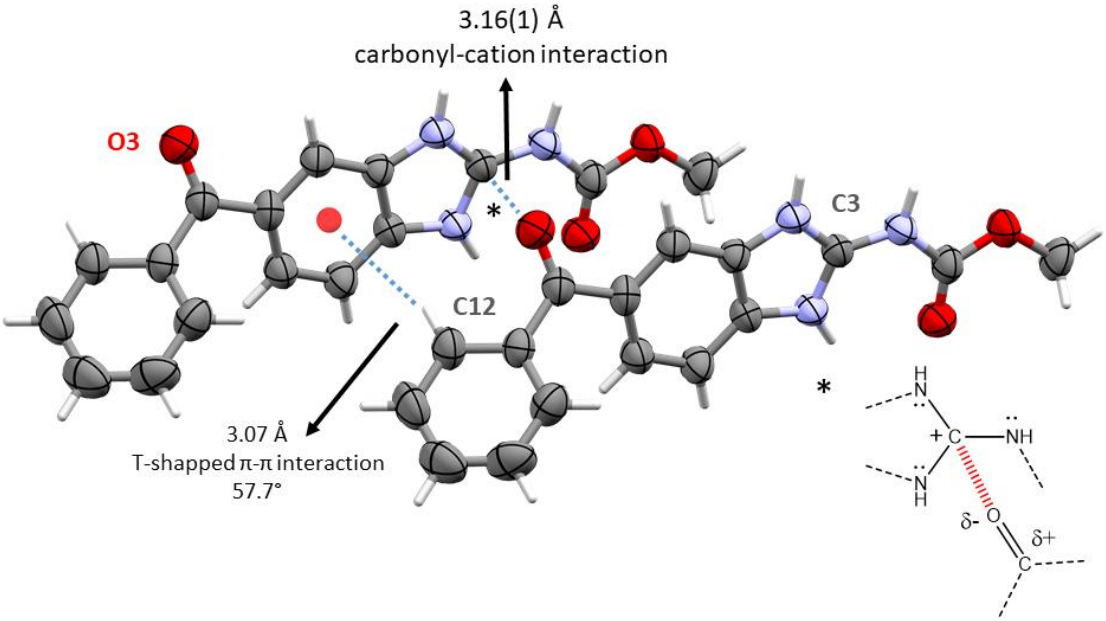

Figure S7. The T-shaped or edge-to-face π···π and the carbonyl···π interactions found in the ac plane of the structure of MBZH·MsO.

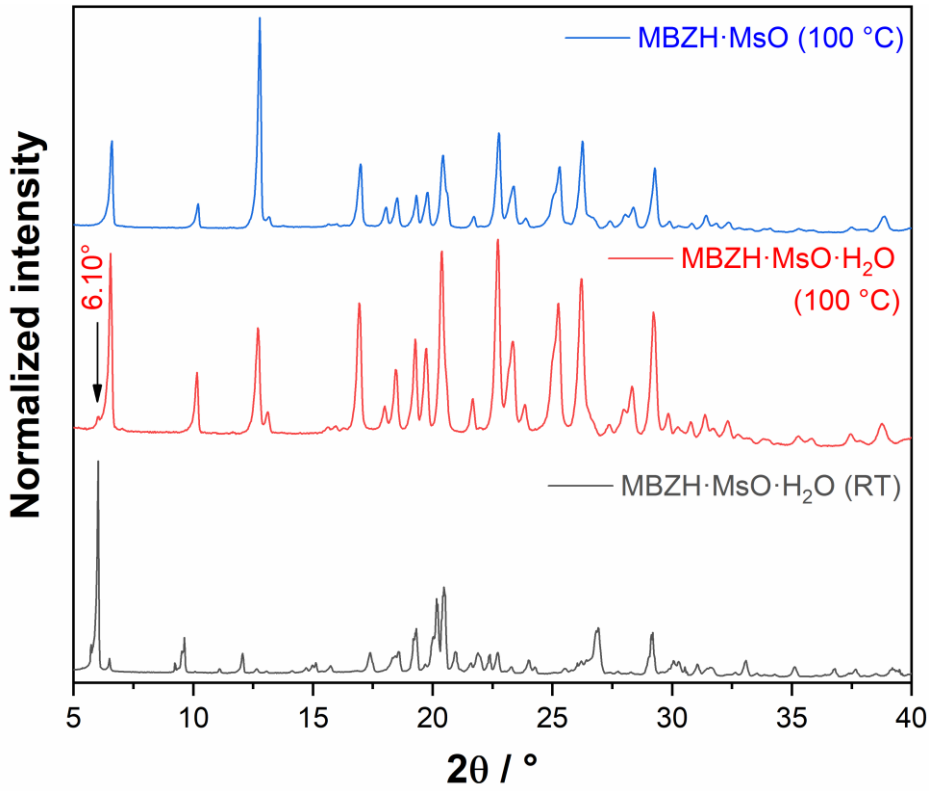

Figure S8. Experimental powder X-ray diffraction patterns of a sample of MBZH·MsO·H_2O at room temperature (RT) (black) and after being kept at 100 °C for 60 min (red) compared to the one of MBZH·MsO in the same conditions (blue).

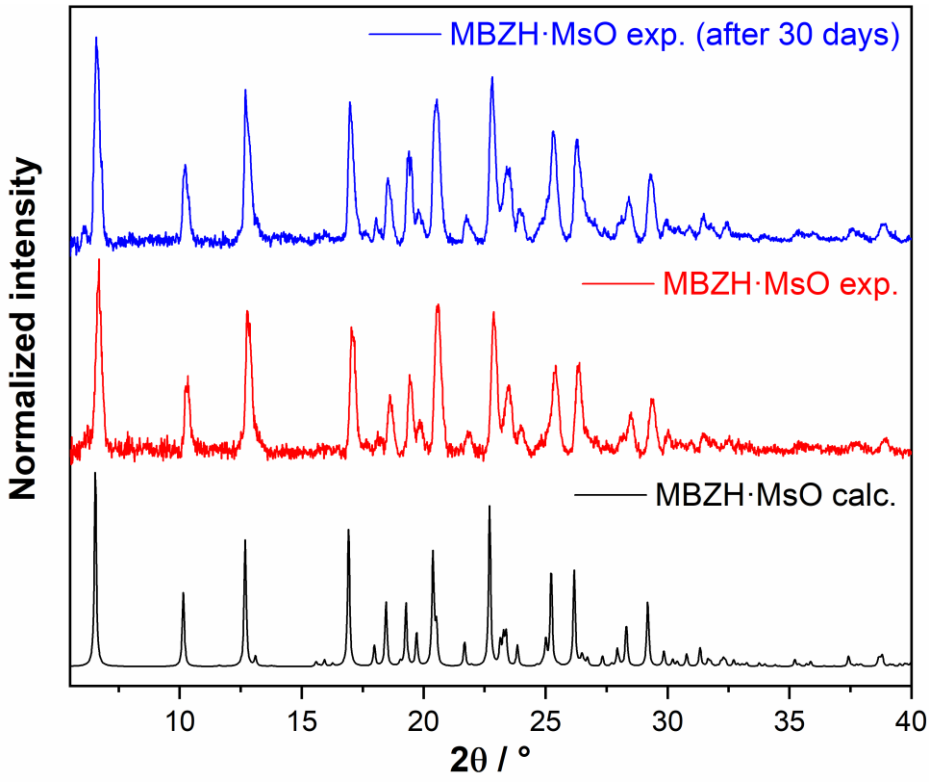

Figure S9. Experimental powder X-ray diffraction patterns of MBZH·MsO recently synthesized and after 30 days in contact with the atmosphere, compared to the one calculated from the solved structure of the MBZH·MsO monohydrate salt.

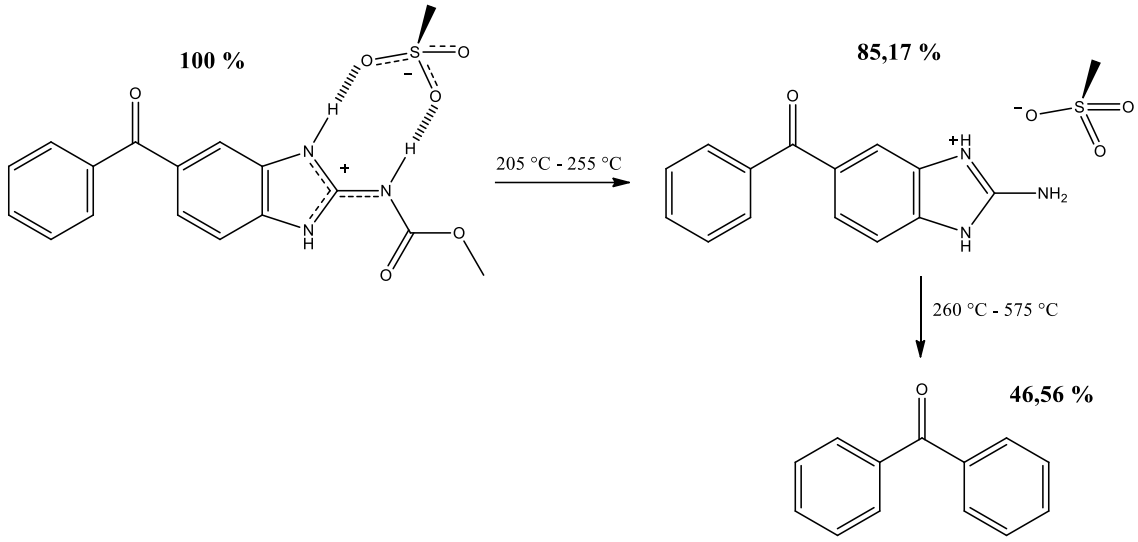

Scheme S5. Proposed mechanisms for MBZH·MsO thermal degradation.

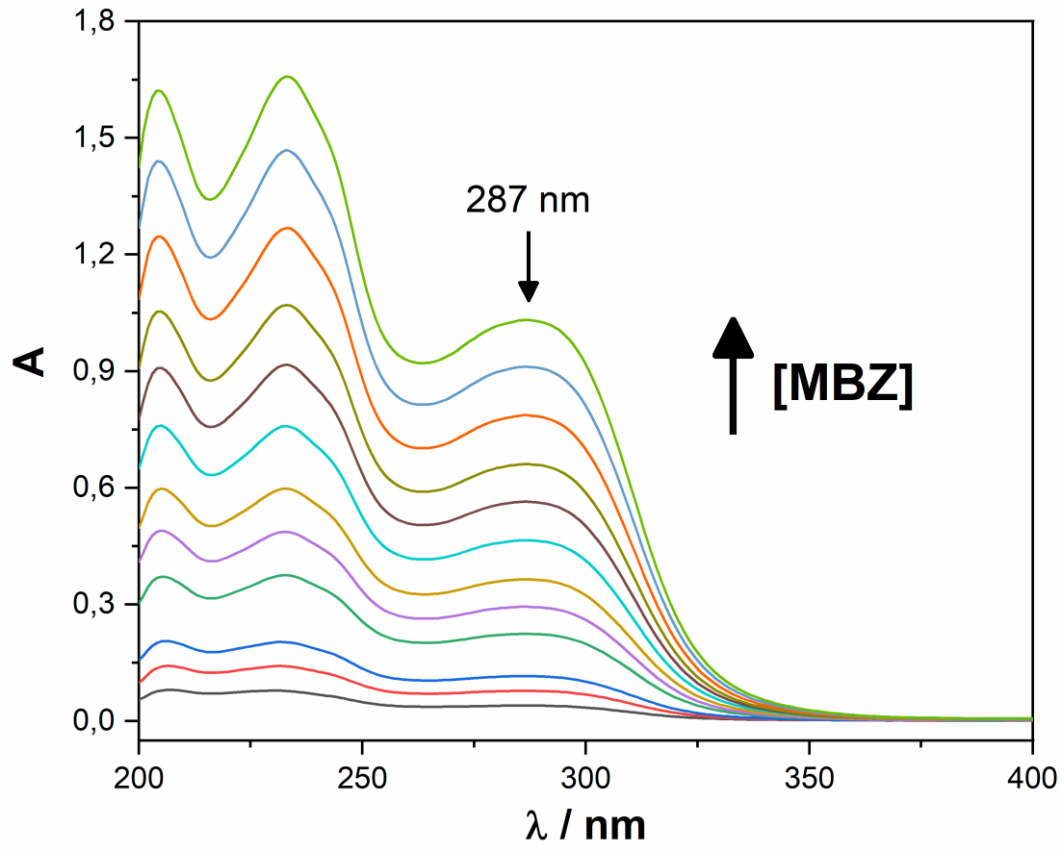

Figure S10. MBZ UV-vis spectra in 0.1 mol L^{-1} hydrochloric acid aqueous solution.

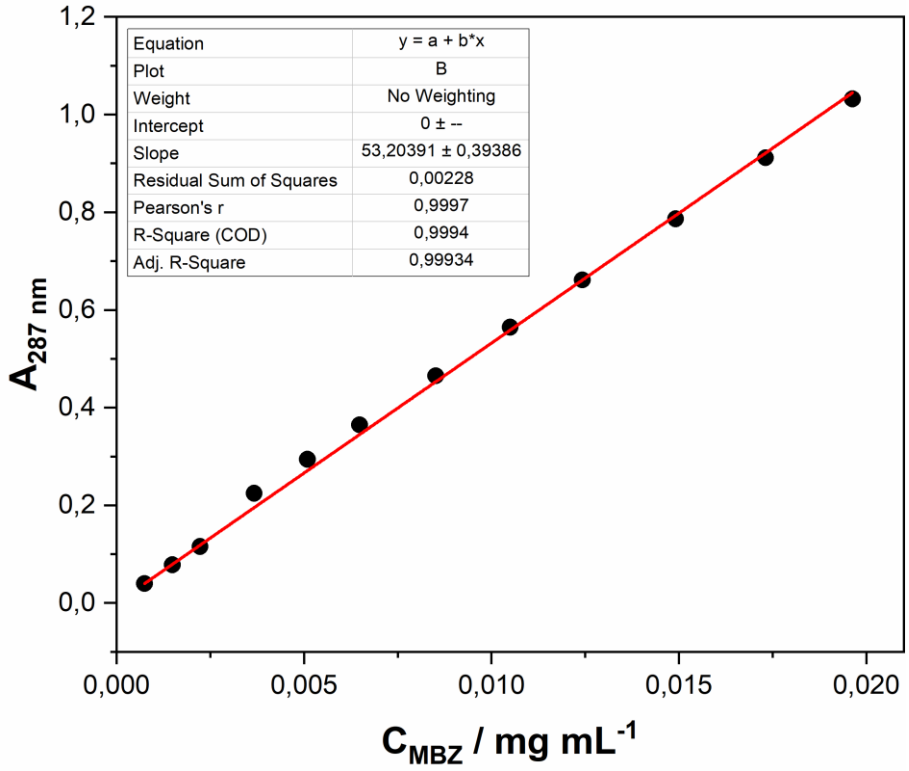

Figure S11. Calibration curve for the quantification of MBZ in 0.1 mol L^{-1} hydrochloric acid aqueous solution.

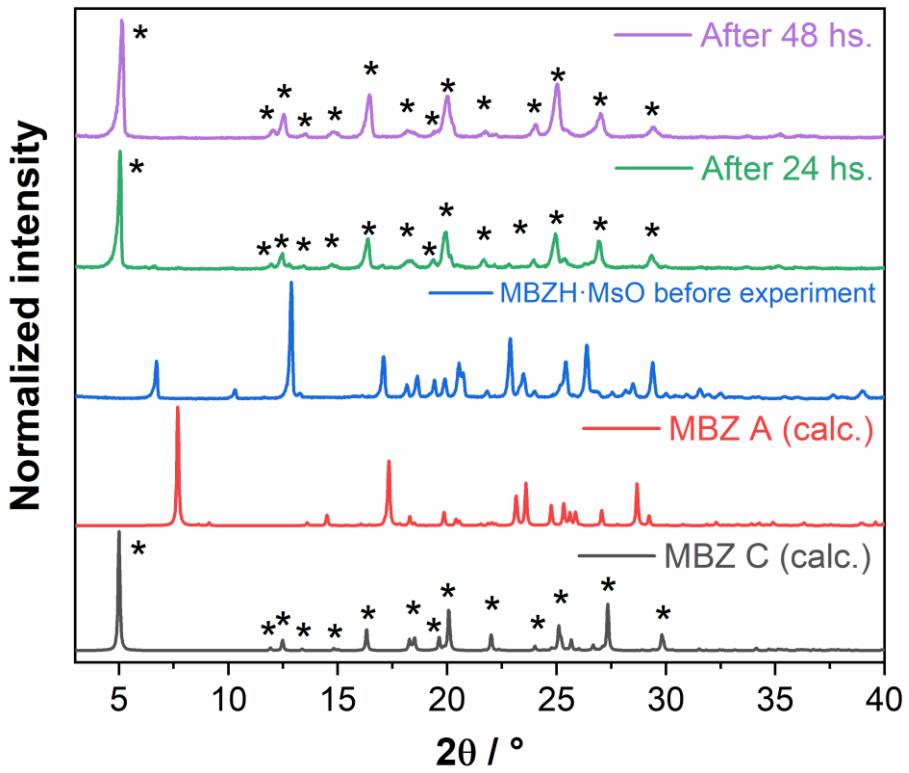

Figure S12. Power X-ray diffraction patters of the solid sediment samples after the solubility experiment, compared with the calculated patterns of MBZ C, MBZ A and MBZH·MsO. (*: MBZ C peaks.)

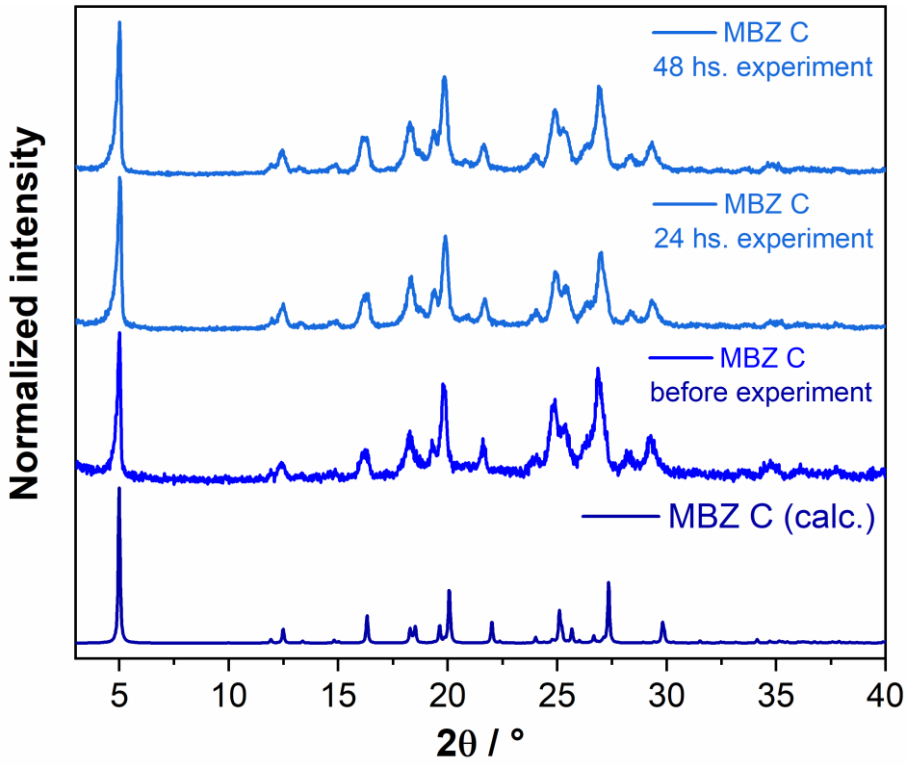

Figure S13. Power X-ray diffraction patters of the MBZ C before and after the solubility experiment, compared to the calculated pattern.

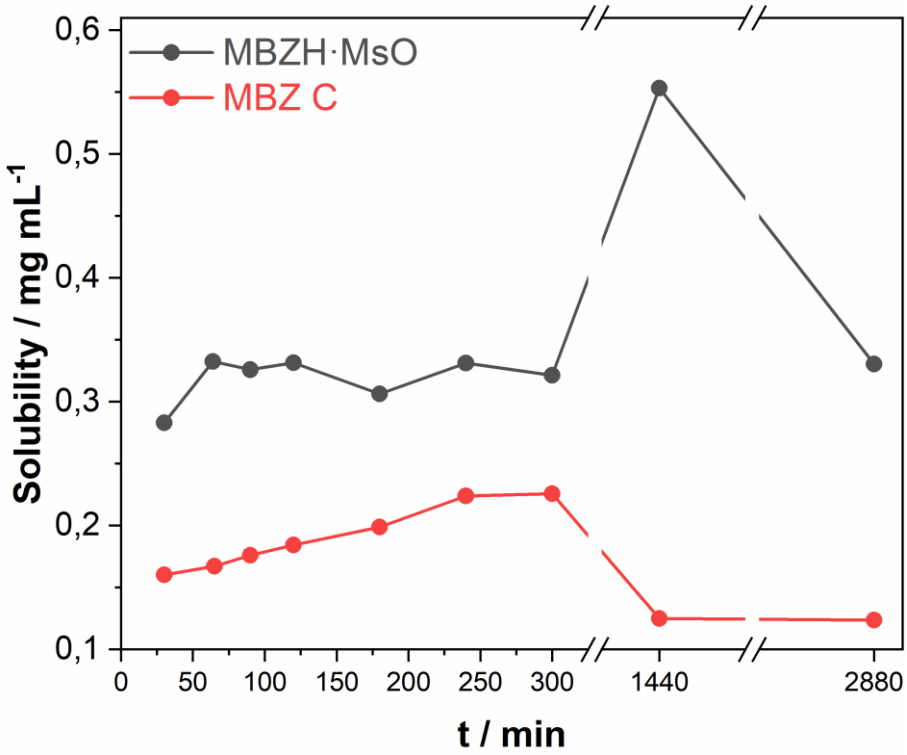

Figure S14. Solubility evolution of MBZH·MsO and MBZ C in 0.1 mol L^{-1} hydrochloric acid aqueous solution.

Bibliography

1 E. L. Gutiérrez, M. S. Souza, L. F. Diniz and J. Ellena, *J. Mol. Struct.*, 2018, **1161**, 113–121.

2 E. L. Gutiérrez, A. A. Godoy, G. E. Narda and J. Ellena, *CrystEngComm*, 2020, **22**, 6559–6568.

3 J. Chen and T. Lu, *Chinese J. Chem.*, 2013, **31**, 635–640.

4 J.-M. Chen, Z.-Z. Wang, C.-B. Wu, S. Li and T.-B. Lu, *CrystEngComm*, 2012, **14**, 6221.

5 K. de Paula, G. E. Camí, E. V. Brusau, G. E. Narda and J. Ellena, *J. Pharm. Sci.*, 2013, **102**, 3528–3538.